Electronic Supplementary Information

Enabling both ultrahigh initial Coulombic efficiency and superior stability of $Na_2Ti_3O_7$ anode via optimizing binders

Ying Li,[a] Yihua Liu,[a] Dong Wang,[a] Changyan Hu,[a] Kangying Luo,[a] Benhe Zhong,[a] Yan Sun,[b] Yang Liu,[c] Zhenguo Wu*[a] and Xiaodong Guo*[a]

[a]*School of Chemical Engineering, Sichuan University, Chengdu 610065, China*

[b]*School of Mechanical Engineering, Chengdu University, Chengdu 610106, China*

[c]*School of Materials Science and Engineering, Henan Normal University, XinXiang 453007, China*

Address correspondence to

Zhenguo Wu, zhenguowu@scu.edu.cn;

Xiaodong Guo, xiaodong2009@ scu.edu.cn

Experimental details

Materials synthesis

$Na_2Ti_3O_7$ (NTO) microrods were prepared by high-temperature solid-state method. 1.02g of Na_2CO_3 (99%, KESHI) and 2.20g of TiO_2 (99%, KESHI), corresponding to a slight excess of Na_2CO_3 with regard to the molar stoichiometry, together with about 3mL ethanol (AR, KESHI) were hand-milled for 30 mins . Then, the well-mixed powder was calcined in air at 900 °C for 15 h with heating and cooling rate of 5 °C min^{-1}. All the original materials were purchased and used without further purification.

The active materials (70 wt%) and SuperP conductive agent (20 wt%) were homogeneously mixed with binder (10 wt%) in corresponding solvent (PVDF corresponding to N-methyl pyrrolidone (NMP); CMC and CMC&SBR corresponding to water) for 0.5 h to form a viscous slurry, which was then casted onto a copper (Cu) foil. After vacuum-drying at 80 °C for 12 h accompanying with the solvent deeply volatilizing, the electrodes were punched into circular pieces with a diameter of 14 mm and mass loading of 3.2±0.3 mg.

Materials characterization

XRD (Bruker D8 Advance, Cu Kα radiation) was carried out to obtain the crystal structure. Scanning electron microscopy (SEM, FEI Inspect F50) and transmission electron microscopy (TEM, JEOLJEM 2100F) images were obtained to identify morphology and microstructure. Raman spectra were collected by using a solid-state 532 nm excitation laser. X-ray photoelectron spectroscopy (XPS, Thermo Scientific K-Alpha+, Mono Al Kα radiation) was used to analyze the SEI film components.

Microscratch test

The bond strength between the electrode-membrane and the copper foil and the cohesive strength between the $Na_2Ti_3O_7$ microrods with conductive carbon particles and the binder were measured by scratching the film surface with a tip of durometer indenter (Rockwell type). A tapered diamond stylus (Berkovich) with a tip radius of 100 μm and a taper angle of 142.3° was used. The scratch tip was placed over the film surface and a 2-mm-long scratch trajectory was made by parallel transporting the sample while linearly increasing the normal load of the tapered tip from 0.01 N to 5 N. Accompanying by normal load rate of 9.98 N min^{-1}, the speed of sample translation was 4 mm s^{-1}. During scratching processes, the tangential force Ft and the normal force Fn were detected on-site in real time.

Electrochemical test

Using these electrode pieces, electrolyte (1.0 M $NaPF_6$ dissolved in glyme i.e., DME), pure sodium foils as counter electrodes and Whatman GF/D glass fibers as separators, 2025-type coin cells were assembled in an argon-filled glove box with both oxygen and moisture contents less than 0.1 ppm. Galvanostatic charge/discharge measurements at different current densities were carried out on a battery controlling system (Neware BTS-610) in a voltage range from 2.5 to 0.01 V (versus Na/Na^+). Cyclic voltammetry (CV) tests were performed on an electrochemical workstation (LK 9805) with a voltage window of 0.01–2.5 V at various scan rates. Electrochemical impedance spectroscopy (EIS) measurements were carried out by Zennium IM6 electrochemical workstation. The galvanostatic intermittent titration technique (GITT) tests were performed on a CT2001A LANHE electrochemical workstation by applying a constant current flux (17.7 mA g^{-1}) for 10 minutes, followed by open-circuit equilibration time for 1.0 h. Diffusion coefficient values are calculated from GITT curves. All the electrochemical measurements above were conducted at 25 °C.

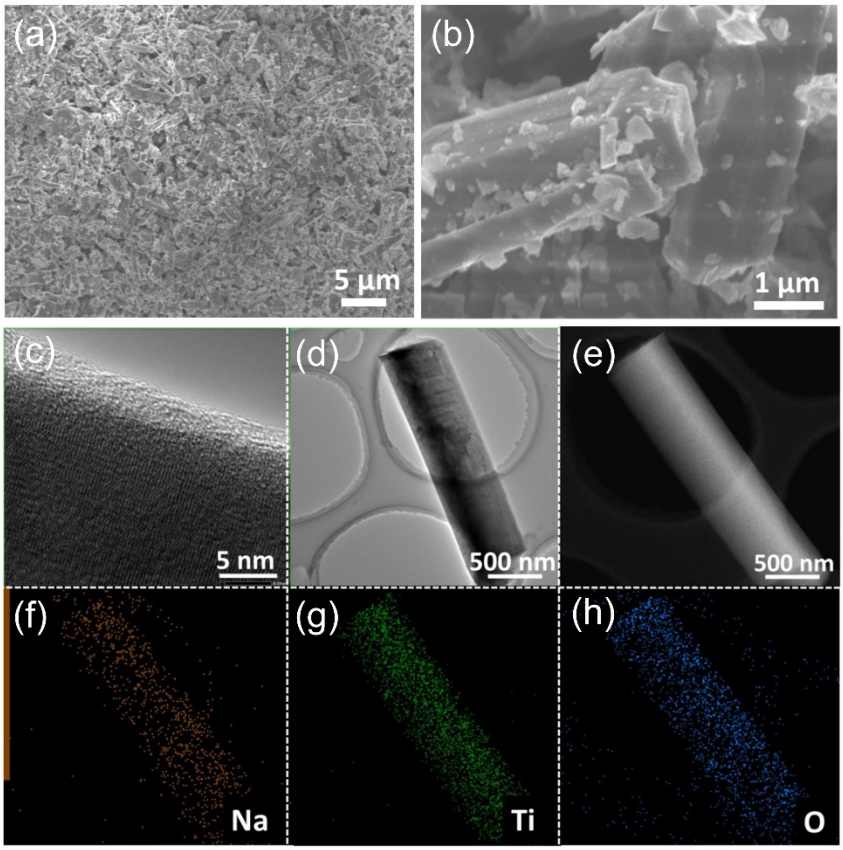

Figure S1 Basic information for the pristine $Na_2Ti_3O_7$ sample. (a) Low magnification and (b) high magnification SEM images, (c-e) TEM and HRTEM images, (f-h) corresponding EDX mapping images.

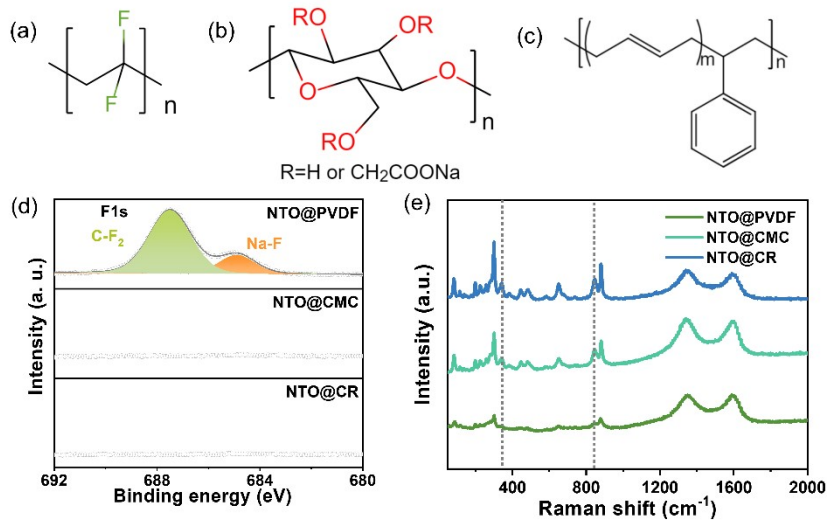

Figure S2 Molecular structural formula of (a) PVDF, (b) CMC and (c) SBR; (d) *F*1s spectra of pristine electrodes; (e) Raman spectra of NTO composite electrodes after one cycle**.**

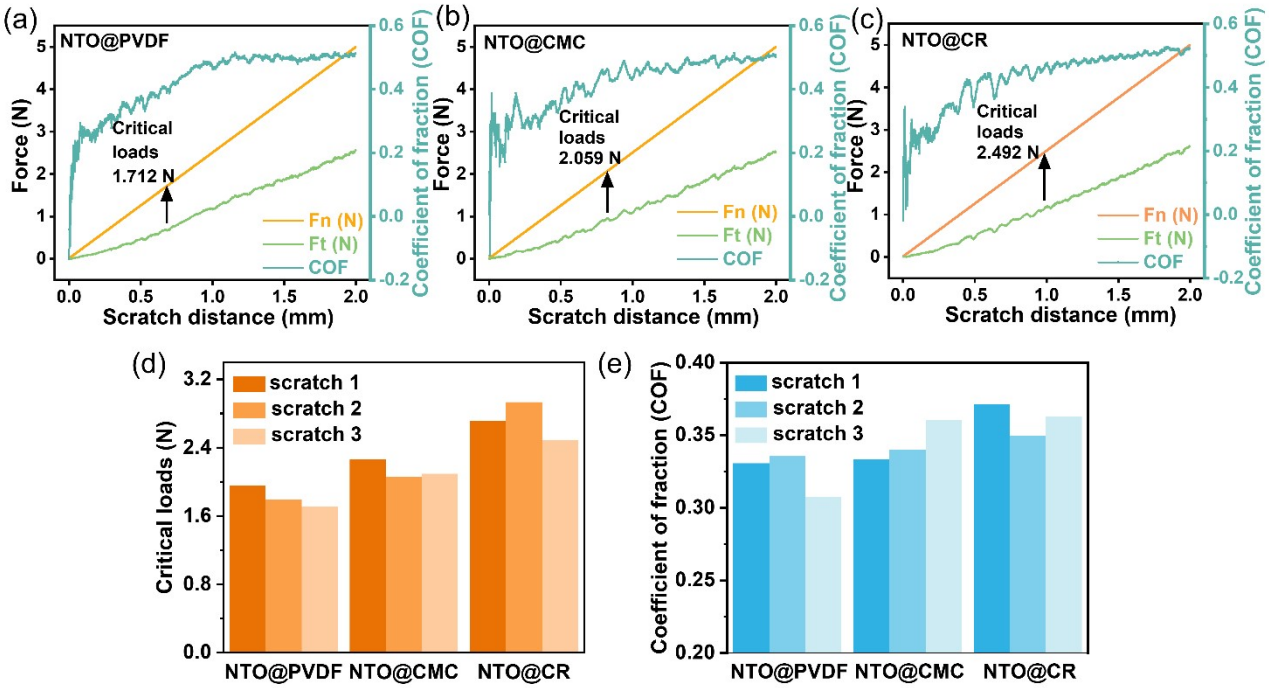

Figure S3 Microscratch test results. Values (*F*n, *F*t, and *COF*) as a function of scratch distance for one of the (a) NTO@PVDF, (b) NTO@CMC and (c) NTO@CR electrodes. (d) Critical loads detected and (e) and *COF*s calculated for each test.

Initially, as the tip started to slide and press on the film surface, the *COF* of all electrodes increased promptly with increasing normal load; and then with the normal load progressively gaining, the *COF* reached steady state and fluctuated slightly; after exceeding the critical delamination load, the *COF* suddenly increased due to the accumulation of obvious delamination debris at the scratch tip.

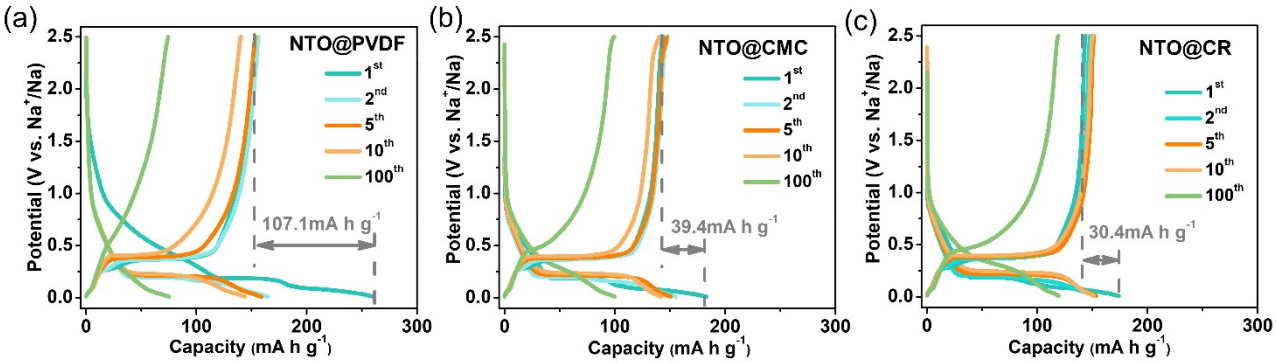

Figure S4 Charge-discharge plots cycled at 0.5 C of (a) NTO@PVDF, (b) NTO@CMC and (c) NTO@CR electrode.

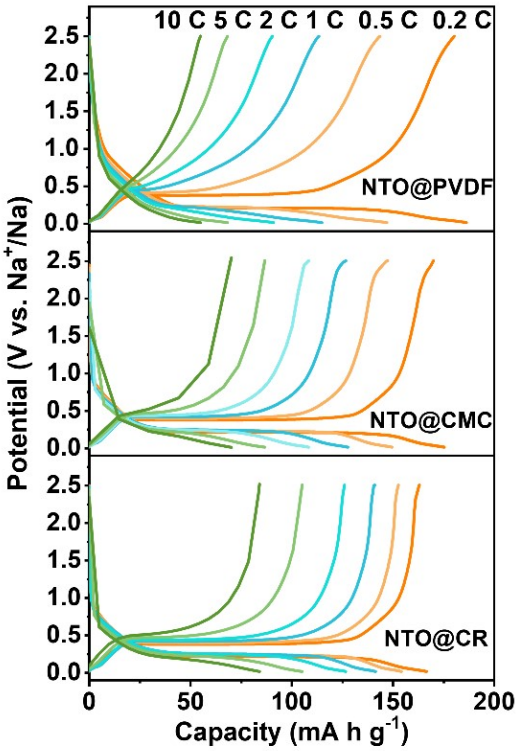

Figure S5 Comparison of charge-discharge plots cycled at different current values.

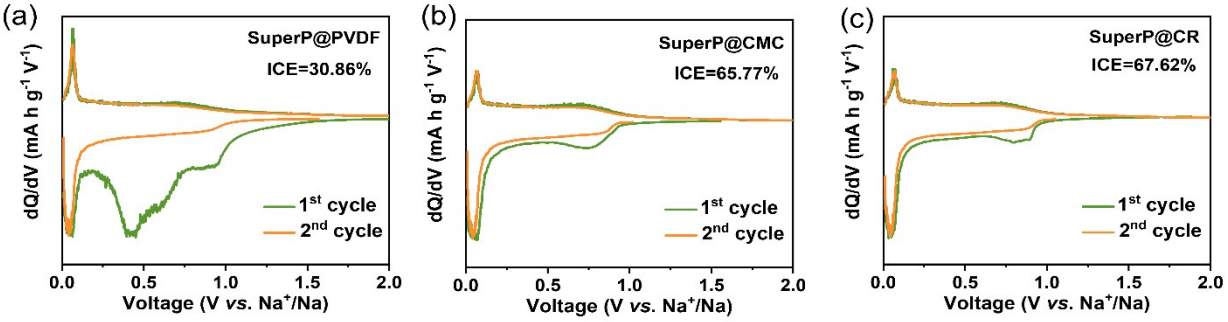

Figure S6 The dQ/dV plots for the first two cycles of (a) SuperP@PVDF, (b) SuperP@CMC, and (c) SuperP@CR.

Table S1 Voltage segmented capacity table

Number of cycles	Electrode	The discharge capacity of corresponding voltage range (mA h g^{-1})			
		0.01-0.136 V	0.136-0.227 V	0.227-2.0 V	0.01-2.0 V
Cycle one	NTO@PVDF	80.24	68.55	111.71	**260.5**
	NTO@CMC	84.37	61.41	37.01	**182.79**
	NTO@CR	80.27	58.83	34.91	**174.01**
		The discharge capacity of corresponding voltage range (mA h g^{-1})			
		0.01-0.085 V	0.085-0.227 V	0.227-2.0 V	0.01-2.0 V
Cycle two	NTO@PVDF	23.98	105.98	34.02	**164.52**
	NTO@CMC	20.46	108.16	26.12	**154.86**
	NTO@CR	20.54	105.75	26.93	**153.31**

Table S2 The discharge capacity difference values for two areas

Electrode	The discharge capacity difference value (mA h g^{-1})	
	Area one	Area two
NTO@PVDF	18.83	77.69
NTO@CMC	17.16	10.89
NTO@CR	12.81	7.98

Table S3 XPS spectral features for electrodes after one cycle

Electrode	Element	Binding Energy (eV)	Peak Assignment	Species
NTO@PVDF	C1s	284.84	C-C	SuperP
		286.27	C-O	R-O-Na
		290.00	C-O_3	Na_2CO_3
	Na1s	1071.5	Na-F, Na-O	NaF, R-O-Na, Na_2CO_3
		1073.22	Na_xPF_y	Na_xPF_y
	F1s	684.63	Na-F	NaF
		687.10	Na_xPF_y	Na_xPF_y
NTO@CMC	C1s	284.86	C-C	SuperP
		286.16	C-O	R-O-Na, CMC
		289.01	C-O_2	CMC
		289.95	C-O_3	Na_2CO_3
	Na1s	1071.27	Na-F, Na-O	NaF, R-O-Na, Na_2CO_3, CMC
	F1s	683.90	Na-F	NaF
		687.39	Na_xPF_y	Na_xPF_y
NTO@CR	C1s	284.90	C-C	SuperP
		286.24	C-O	R-O-Na, CMC
		289.23	C-O_2	CMC
		290.06	C-O_3	Na_2CO_3
	Na1s	1071.50	Na-F, Na-O	NaF, R-O-Na, Na_2CO_3, CMC
	F1s	683.68	Na-F	NaF
		687.64	Na_xPF_y	Na_xPF_y

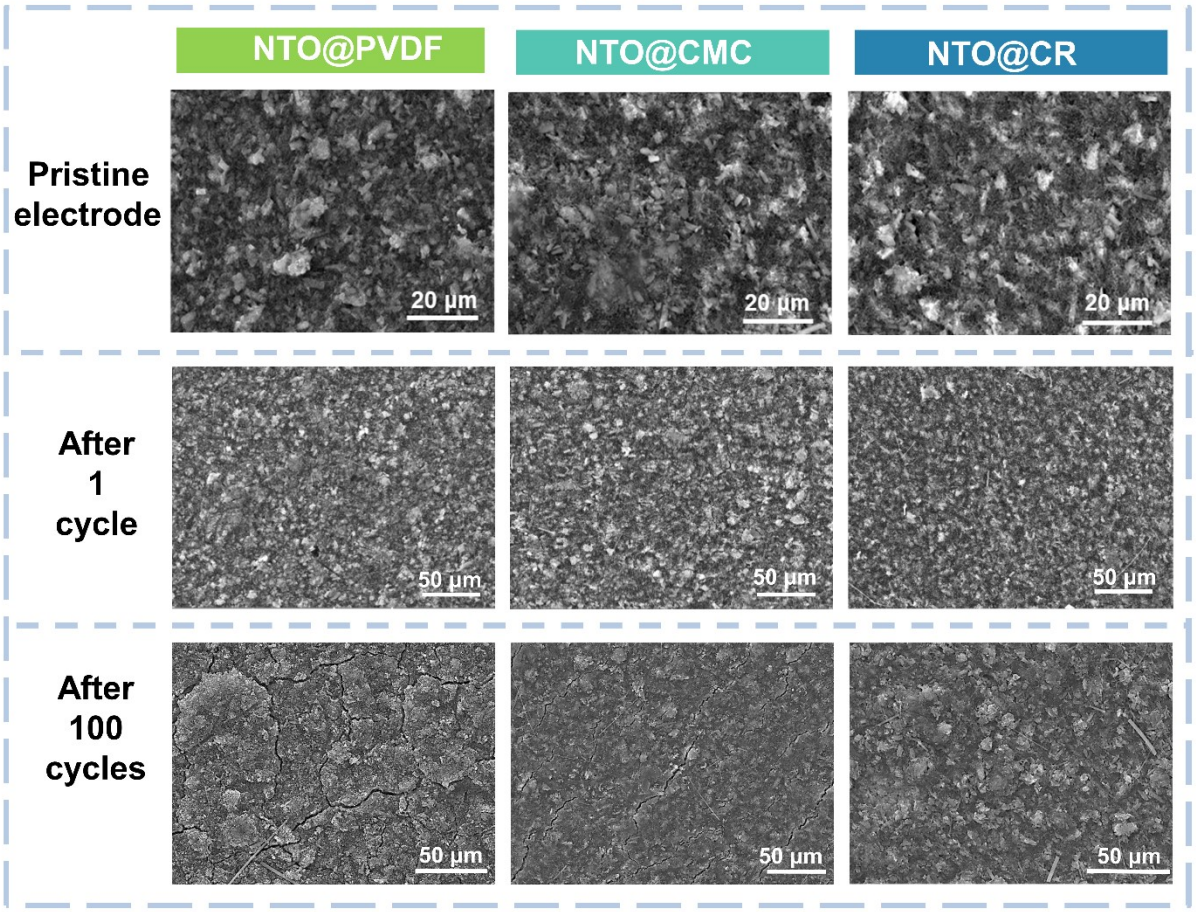

Figure S7 SEM images of (a-c) pristine electrodes, (d-f) electrodes after 1 cycle and (c) after 100 cycles.

Table S4 XPS spectral features for NTO@PVDF electrode after 100 cycles

Element	Depth	Binding Energy (eV)	Peak Assignment	Peak Area (CPS.eV)	Species
F1s	0 nm	685.70	Na-F	7070.901	NaF
		687.93	Na_xPF_y	79680.18	Na_xPF_y
	17 nm	685.91	Na-F	29355.26	NaF
		687.70	Na_xPF_y	73674.58	Na_xPF_y
	117 nm	685.87	Na-F	85699.82	NaF
		687.4	Na_xPF_y	35642.8	Na_xPF_y
Na1s	0 nm	1073.38	Na-F, Na-O	244155.2	NaF, R-O-Na Na_2CO_3
		1074.69	Na_xPF_y	111722.1	Na_xPF_y
	17 nm	1073.44	Na-F, Na-O	344880.8	NaF, R-O-Na Na_2CO_3
		1074.53	Na_xPF_y	219262	Na_xPF_y
	117 nm	1073.01	Na-F, Na-O	451643	NaF, R-O-Na Na_2CO_3
		1074.19	Na_xPF_y	101184.7	Na_xPF_y

Element	Depth	Binding Energy (eV)	Peak Assignment	Peak Area (CPS.eV)	Species
C1s	0 nm	284.83	C-C	54693.66	SuperP
		286.37	C-O	52461.48	R-O-Na
		290.42	C-O_3	14221.4	Na_2CO_3
		291.7	C-F_2	16682.66	PVDF
	17 nm	284.98	C-C	49917.45	SuperP
		286.36	C-O	33503.4	R-O-Na
		290.69	C-O_3	7284.991	Na_2CO_3
		291.69	C-F_2	18228.49	PVDF
	117 nm	284.91	C-C	53090.7	SuperP
		286.2	C-O	35110.77	R-O-Na
		290.6	C-O_3	5082.72	Na_2CO_3
		291.51	C-F_2	9998.086	PVDF

Table S5 XPS spectral features for NTO@CMC electrode after 100 cycles

Element	Depth	Binding Energy (eV)	Peak Assignment	Peak Area (CPS.eV)	Species
F1s	0 nm	685.32	Na-F	8686.476	NaF
		688.32	P-F	6037.77	Na_xPF_y
	17 nm	685.38	Na-F	12503.31	NaF
		688.12	P-F	4478.88	Na_xPF_y
	117 nm	685.35	Na-F	19308.55	NaF
		687.99	P-F	2744.663	Na_xPF_y
Na1s	0 nm	1073.05	Na-F, Na-O	300974.8	NaF, R-O-Na Na_2CO_3, CMC
	17 nm	1073.07	Na-F, Na-O	361738.5	NaF, R-O-Na Na_2CO_3, CMC
	117 nm	1072.95	Na-F, Na-O	316988.7	NaF, R-O-Na Na_2CO_3, CMC
C1s	0 nm	284.70	C-C	67748.59	SuperP
		285.83	C-O	29446.84	R-O-Na, CMC
		287.29	C-O_2	32674.44	CMC
		290.57	C-O_3	22188.33	Na_2CO_3
	17 nm	284.66	C-C	62764.25	SuperP
		285.78	C-O	33108.65	R-O-Na, CMC
		287.22	C-O_2	27659.34	CMC
		290.77	C-O_3	19154.61	Na_2CO_3
	117 nm	284.67	C-C	65819.7	SuperP
		285.72	C-O	39052.81	R-O-Na, CMC
		287.29	C-O_2	28672.27	CMC
		290.75	C-O_3	16619.2	Na_2CO_3

Table S6 XPS spectral features for NTO@CR electrode after 100 cycles

Element	Depth	Binding Energy (eV)	Peak Assignment	Peak Area (CPS.eV)	Species
F1s	0 nm	684.94	Na-F	2738.095	NaF
		688.16	P-F	12066.78	Na_xPF_y
	17 nm	685.21	Na-F	9322.888	NaF
		688.26	P-F	5708.628	Na_xPF_y
	117 nm	685.32	Na-F	37757.95	NaF
		687.94	P-F	13338.45	Na_xPF_y
Na1s	0 nm	1072.80	Na-F, Na-O	137106.7	NaF, R-O-Na Na_2CO_3, CMC
	17 nm	1072.89	Na-F, Na-O	191000.5	NaF, R-O-Na Na_2CO_3, CMC
	117 nm	1072.81	Na-F, Na-O	187401.7	NaF, R-O-Na Na_2CO_3, CMC
C1s	0 nm	284.80	C-C	126439.1	SuperP
		285.70	C-O	67444.31	R-O-Na, CMC
		287.13	$C-O_2$	22727.78	CMC
		289.90	$C-O_3$	14745.21	Na_2CO_3
	17 nm	284.78	C-C	117330.9	SuperP
		285.78	C-O	63479.4	R-O-Na, CMC
		287.15	$C-O_2$	26698.17	CMC
		290.51	$C-O_3$	12521.9	Na_2CO_3
	117 nm	284.69	C-C	121970.8	SuperP
		285.63	C-O	59941.81	R-O-Na, CMC
		286.84	$C-O_2$	20947.02	CMC
		289.62	$C-O_3$	31757.97	Na_2CO_3

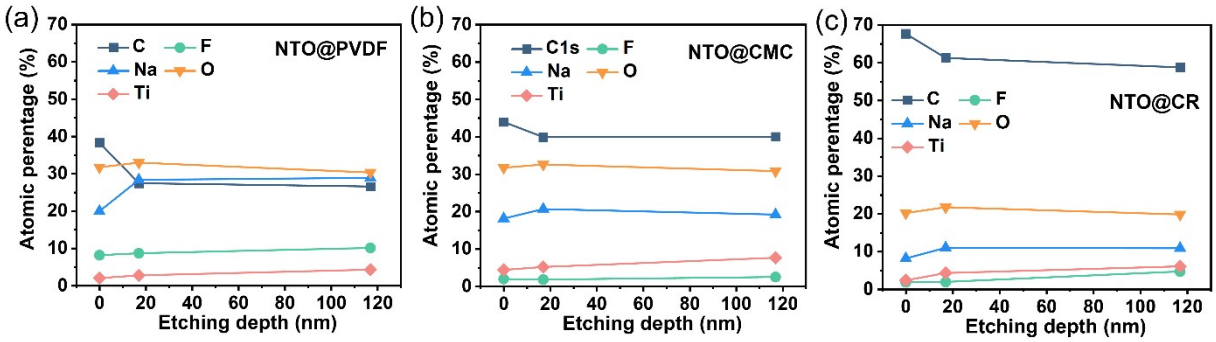

Figure S8 Relative content of each element Changes within etching depth for (a) NTO@PVDF, (b) NTO@CMC and (c) NTO@CR electrode after 100 cycles.

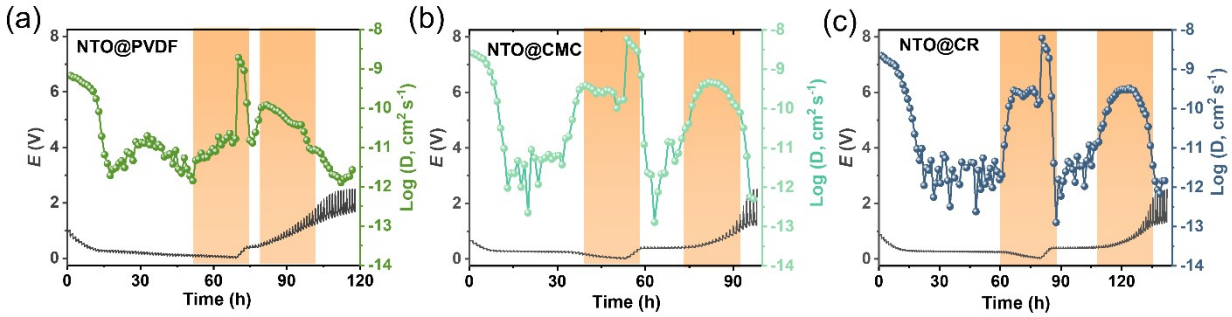

Figure S9 Galvanostatic intermittent titration technique (GITT) potential profiles and Na^+ apparent diffusion coefficients calculated from the GITT potential profiles of (a) NTO@PVDF, (b) NTO@CMC and (c) NTO@CR electrode after 10 cycles.